Received 26 June 2022, accepted 10 July 2022, date of publication 13 July 2022, date of current version 20 July 2022.
Digital Object Identifier 10.1109/ACCESS.2022.3190710

RESEARCH ARTICLE

Pre-Perturbation Operational Strategy Scheduling in Microgrids by Two-Stage Adjustable Robust Optimization

MILAD MANSOURI[1], MOHSEN ESKANDARI[2], YOUSEF ASADI[1], PIERLUIGI SIANO[3,4], (Senior Member, IEEE), AND HASSAN HAES ALHELOU[5], (Senior Member, IEEE)
[1]Department of Electrical Engineering, Bu-Ali Sina University, Hamedan 65168 63611, Iran
[2]School of Electrical Engineering and Telecommunications, University of New South Wales, Sydney, NSW 2052, Australia
[3]Management and Innovation Systems Department, Salerno University, 84084 Salerno, Italy
[4]Department of Electrical and Electronic Engineering Science, University of Johannesburg, Johannesburg 2006, South Africa
[5]Department of Electrical and Computer System Engineering, Monash University, Clayton, VIC 3800, Australia
Corresponding author: Hassan Haes Alhelou (alhelou@ieee.org)

ABSTRACT A two-stage adaptive robust optimization is developed for pre-disturbance scheduling in microgrids (MGs) for handling uncertainties associated with electricity market prices, renewable generation, demand forecasts, and islanding events. The objective is to produce a reliable and optimal solution for MG operation that minimizes operational costs and the risk/failure in islanding events. In the literature, the uncertainty sets associated with islanding events cover a full scheduling period which results in a sub-optimal solution. In this paper, uncertainty sets corresponding to islanding events are modeled based on reliability/resiliency-oriented indexes of the MG/grid to achieve a more accurate/reliable solution. Besides, the Benders decomposition algorithm which is used to handle uncertainties in solving the optimization problem is time-consuming. Therefore, the column-and-constraint generation (C&CG) decomposition strategy is adopted to make the problem computationally tractable. Further, the uncertainty budget parameters are clarified to balance the conservatism and optimality (cost minimization) of the robust solution in uncertainty sets. The effectiveness of the proposed framework is evaluated and discussed by using a set of numerical studies with different scenarios in an MG. The simulations show that the proposed framework reduces operational costs by using the precise analysis of uncertainty budgets and a change in scheduling periods.

INDEX TERMS Energy management system, energy storage systems, microgrid, pre-disturbance scheduling, renewable energy resources, robust optimization, uncertainty.

I. INTRODUCTION

A microgrid (MG) is a small-scale electric grid comprising distributed energy resources (DERs) and local loads [1]. MGs operate in two grid-connected or islanded operating modes [2]. The grid-connected MG exchanges power with the main grid, which could be from the grid to the MG or vice versa. Also, the MG should be able to be disconnected from the grid to continuously support its local loads by DERs within the MG [3].

A hierarchical control system is adopted in MGs to handle dynamic performance and economic programs for the stable and efficient operation of the MG in different operating modes. At the highest level of the MG control system, the energy management system (EMS) runs optimization-based programs to minimize costs of power production and maximize MG revenues.

Various optimization methods, either problem-based or solver-based approaches, such as distributed stochastic/robust optimization [4], multi-stage optimization [5], [6], multi-objective optimization [7], fuzzy approach [8], [9], heuristic and evolutionary methods [10], neural network [11],

The associate editor coordinating the review of this manuscript and approving it for publication was Lei Wang.

convex robust programming [12], bi-level robust optimization [13], etc., are used to handle EMS problems [14], [15].

However, uncertainties associated with the generated power by renewable energy resources (RESs), load profile, and electricity tariffs cause tremendous challenges for EMS to achieve a more optimal/reliable solution [16]. Optimization approaches for managing uncertainties can be classified into two main categories: stochastic programming and robust optimization. The stochastic programming approach is scenario-centric and considers probability distribution function (PDF) for uncertain parameters [17]. Then, the Monte Carlo method is used to simulate scenarios based on the distribution function and the probability of each scenario is determined to calculate the probability of occurrence of each scenario [18]. Robust optimization is practical when the uncertainty sets of uncertain parameters/variables are available. This eliminates the requirement of generating the corresponding probability distribution to a parameter by accessing historic data. Also, it is not necessary to define an unrealistic PDF [19], which reduces the risk level.

Robust optimization can be implemented using single-stage robust programming or through multi-stage robust programming. In single-stage robust optimization, the optimal values of the decision variables are obtained in one step and are not adjustable based on the amount of uncertainty, which may make them too conservative [20]. When the energy management system involves uncertainty, it becomes an NP-hard problem and it is not possible to solve this problem in the polynomial time. The optimal solution to the decision variables can not be obtained at one stage, otherwise, the solution would be too conservative and sub-optimal. Multi-stage approaches are considered. The first stage is planned to adjust the value of the problem variables and the second stage is planned to obtain the optimal value of these uncertain parameters. In each iteration, by specifying the values of the second variables, it can be entered as a known parameter in the first stage by the algorithm and the optimal values of the variables in the first stage are obtained [5]. However, multiple-stage robust optimization problems are difficult to be programmed and computed.

For example, some of the advances in recent studies using the robust optimization approach are reviewed as follows: In [21], a multi-level robust optimization model for solving the dispatching problem in microgrids is presented. In the first level of this approach, the operating cost of the microgrid and in the second level, the load shedding are minimized. The novel nested reformulation-and-decomposition (R&D) algorithm is used to solve the multi-level optimization problem. A hierarchical frequency control structure is presented in the form of a two-level robust optimization approach [22]. At the first level, that approach seeks to minimize the operating cost of the microgrid. To solve the introduced model, the column and constraint generation algorithm is used. The power exchange programmed in multi- microgrids using the two-level adjustable robust optimization approach is mentioned in [23]. In the first level, the generated and exchanged power between buses AC and DC is obtained and the column and constraint generation algorithm is used to solve the model.

To summarize, the significant shortcomings observed in the existing works of energy management via robust optimization in MGs are classified as follows:

1) One solution to make the robust optimization tractable is to use approximation algorithms such as Benders decomposition (BD) [24]. The strategy behind the BD algorithm is to form a secondary objective function through duality solutions. However, there are significant issues with the BD algorithm such as a large number of iterations and computational time to achieve the optimal solution. The column and constraint generation (C&CG) algorithm [25] is more efficient than BD [26], which has been less utilized in MGs EMS problems, as it can solve the master problem with a higher number of variables and more constraints. The number of iterations for this algorithm is much smaller than those of the BD. The BD algorithm uses different methods for achieving feasibility and optimality in terms of cut generation, while in the C&CG algorithm, a unified approach is used for simultaneously generating these cuts, which simplifies the computations. In the BD algorithm, the sub-problem should be a linear model, whereas, in the C&CG algorithm, it could be arbitrary depending on the type of variables.
2) In adjustable robust optimization models, the worst-case scenarios occur at the lower bounds (LB) or upper bounds (UB) of uncertain parameters. Under these circumstances, the resulting solution seems to be more conservative than the stochastic approach [27]. To address this issue, uncertainty budgets are defined in uncertainty sets to limit the number of hours that an uncertain parameter value can approach its UB or LB limit. By selecting the appropriate value of uncertain parameters, the economic efficiency of the robust optimization approach can be significantly improved. In this sense, the drawback of previous studies in [6] and [28] is the lack of using an efficient technique to determine the more optimal amount of uncertainty budget. Besides, the effect of the value of each uncertainty budget on the optimal value of the objective function is not clarified.
3) The uncertainties associated with the MG islanding can be identified based on two indexes: *i*) reliability of the local (micro) grid (such as maintenance and failure rates, etc.), and *ii*) resiliency of the main grid as a global index (e.g., due to climate events and natural disasters). Also, the other difference between the two categories is the time scale, which should be considered for uncertainty sets modeling. In modeling the reliability-based uncertainty, a full-time horizon (i.e., 24 hours) can be considered. On the other hand, for modeling uncertainties associated with resiliency-based islanding, a shorter interval (e.g., 6 hours) can be considered based

on the weather forecast. Taking these two sets of uncertainties and bounding the resiliency-based uncertainty interval can help to achieve more accurate and optimal results. However, this issue has not been considered in the existing works [16], [29].

4) In most robust optimization approaches, uncertainties are modeled as interval, polyhedron, or discrete uncertainty sets in the problem. Alternatively, in the multi-stage approaches, these sets can be considered as auxiliary decision variables in the second stage, which result in a smaller number of iterations and faster convergence. However, in the majority of relevant works, the values of these parameters are not indicated [31]–[33]. As a result, there is no guarantee that the parameter values are in defined sets and thus the obtained optimal solution is not reliable/valid.

To address the mentioned shortcomings, this paper provides pre-perturbation scheduling in microgrids to determine the on/off status of the power resources (diesel generators), charge/discharge profile of energy storage systems (ESSs), and the amount of power purchased/sold from/to the main grid in the day-ahead energy market. The problem objectives are minimizing costs associated with fuel-based DERs, maximizing revenues from RESs, and minimizing the risk corresponding to islanding events.

To this end, a two-stage adjustable robust optimization (ARO) approach is implemented to minimize the operational costs of the MGs by considering uncertain parameters. The robust optimization approach is used due to being more practical than the stochastic approach in handling uncertainties in the scheduling state. Further, the column and constraint generation algorithm is used to solve the problem to cope time complexity of conventional methods such as Benders decomposition.

The contributions of this paper are summarized as follows:

1) The problem of pre-perturbation energy management in microgrids is formulated in the form of a two-level adjustable robust optimization approach. We have used three interval uncertainty sets models that have been secured against the worst-case scenarios. The microgrid operator can construct these uncertainty sets without having an unrealistic probability distribution function. Expanding the proposed structure can find robust solutions for first-level decision variables and second-level uncertain parameters that are robust against any realization of uncertainty sets and minimize the undesirable consequences of islanding events.
2) For improving the optimality and accuracy of the optimal solution, a more flexible and accurate model for the uncertainty set associated with the binary parameter indicating the MG islanding event is developed. To this end, islanding uncertainty is set based on the combination of reliability/resiliency indexes of the MG/grid to achieve a more optimal/reliable solution. By receiving accurate information on weather maps and converting the scheduling intervals to shorter intervals with more accuracy, this set of uncertainty prevents further operating costs from being imposed on the microgrid.
3) Uncertainty budget parameters are defined in uncertainty sets to adjust the conservative level of sets. Selecting the appropriate value of these parameters leads to the better economic efficiency of the robust approach than the stochastic approach. We used a different technique to select uncertainty parameters, which have the possibility of occurring with the desired conservative level, which results in a more efficient and reliable solution.
4) To solve the proposed robust approach, the C&CG algorithm is employed, which works based on a two level decomposition. We have improved the convergence speed of the algorithm by placing the energy storage variables in the second level and providing sufficient conditions for eliminating the binary variable associated with the simultaneous charge and discharge of battery through adding related auxiliary constraints in each iteration.
5) Extensive numerical analysis has been done to demonstrate the effectiveness of the two-stage ARO framework. As a result, the analysis has led to the selection of the more optimal and valid solution.

The remainder of this paper is organized as follows: Section II describes the methodology framework. In section III, the modeling of uncertainty sets is discussed. The problem of MG EMS in the framework of robust optimization is modeled in section IV. The effectiveness of the proposed approach is evaluated in Section V, by using a set of numerical studies with different scenarios. Finally, conclusions are drawn in Section VI.

II. METHODOLOGY FRAMEWORK

A. TWO-STAGE ARO MODEL

For the sake of brevity, this paper focuses on a linear model and can be applied to nonlinear models. The functions and decision variables at the first and second stages are considered linear and the uncertainty set model is assumed to be polyhedron or discrete. Let y, x be the column vectors of the first-stage and the second-stage decision variables, respectively, and U be the uncertainty set. The general framework of the two-stage ARO model is given as

$$\min_{y} \left(a^T y\right) + \max_{u\in U} \left(\min_{x\in \mathrm{Z}(y,u)} \left(b^T x\right)\right) \tag{1}$$

$$s.t.\ Ay \geq d, \quad y \in S_y \tag{2}$$

$$\mathrm{Z}(y, u) = \{\mathrm{x} \in S_x : Gx \geq h - Ey - Mu\} \tag{3}$$

where $S_y \subseteq R^{1\times n}$ and $S_x \subseteq R^{1\times m}$, a^T is a matrix of coefficients of first stage variables; b^T is a matrix of coefficients of second stage variables; A and E are matrices of coefficients of first stage variables in constraints, G matrix of coefficients of second stage variables in constraints, M denotes a matrix of coefficients of the uncertain parameter in constraints and, d and h present fixed coefficient matrixes. The innermost maximum-minimum problem ($max\left(min\left(b^T x\right)\right)$) is known as the recourse problem. In the above equation, z includes all the constraints of the second stage. In this section, a different method than BD is used to solve the problem. In this approach, the cutting planes are created by auxiliary variables as a constraint on the auxiliary problem. The whole procedure is a method of producing C&CG. It is initially considered that the set of uncertain parameters is finite and countable. Let equations $U = \{u_1, \ldots, u_r\}$ and $x = \{x_1, \ldots, x_r\}$ be the corresponding recourse decision of r number of variables. Similar to the BD algorithm, this approach is also used in the master-subproblem framework. Then, the two-stage ARO in the above equations can be reformulated as the following equations:

1) MASTER PROBLEM

$$\min_{y,\eta} \left(a^T y\right) + \eta \tag{4}$$

$$s.t.\ Ay \geq d \tag{5}$$

$$\eta \geq b^T x^l, \quad l = 1, \ldots, r \tag{6}$$

$$Ey + Gx^l \geq h - Mu_l, \quad l = 1, \ldots, r \tag{7}$$

$$y \in S_y, \quad x^l \in S_x,\ l = 1, \ldots, r. \tag{8}$$

Therefore, solving a two-stage ARO problem becomes the equivalent of a mixed-integer programming problem.

2) SUB-PROBLEM

The sub-problem leads to the extraction of the optimal solution (u^*, x^*) with a finite value $Q(y)$ or to find values from the uncertainty set based on which the second-stage decision variables are infeasible. Let $Q(y)$ as the following equation:

$$Q(y) = \left\{\max_{u\in U}\left(\min_{x}\left(b^T x\right)\right) | Gx \geq h - Ey - Mu, x \in S_x\right\} \tag{9}$$

B. SOLUTION METHOD

1) C&CG ALGORITHM

In practice, the sum of extreme points which is the product of the members of three uncertainty sets is very high; therefore, solving a model with such a scale would be highly complicated. Solving the model per sub-set of the scenario members will provide a stronger LB for the discussed two-stage model. A stronger LB means that: in the first iteration, the value of the LB is $(-\infty)$, and in each iteration, the value becomes more optimal and reaches a positive number close to the UB. Thus, by adding non-trivial scenarios in each iteration in this sub-set, a stronger LB would be obtained for the model. The C&CG algorithm adds the worst-case scenario to the sub-set in each iteration and the solution process continues until being converged into the optimal solution. The main idea is to use the C&CG algorithm based on these three steps:

- Start each iteration with a subset of the uncertainty sets;
- Add a significant number of non-repetitive scenarios to achieve the optimal solution;
- Create auxiliary decision variables in each iteration as auxiliary constraints and add them to the master problem.

Here, above equations (6-7) model these three steps. The BD algorithm uses different methods for achieving feasibility and optimality in terms of cut generation, while in the C&CG algorithm, a unified approach is used for simultaneously generating these cuts; this simplifies the computations and leads to economic efficiency.

The solution algorithm is as following equations:

1) Placing the initial values of the input parameters as

$$LB = -\infty, \quad UB = +\infty \text{ and, } k = 0$$

2) Solving the master problem, obtaining the optimal solution η^*_{k+1} and y^*_{k+1}, and updating the LB as:

$$max\{LB, a^T y^*_{k+1} + \eta^*_{k+1}\} \tag{10}$$

3) Solving the sub-problem, obtaining the optimal solution of the sub-problem and uncertain parameters to create a new scenario, constructing the relevant constraints, adding them to the master problem in the next iteration, and updating the UB as:

$$min\left\{UB, a^T y^*_{k+1+} Q(y^*_{k+1})\right\} \tag{11}$$

4) Calculating a limit required for stopping the algorithm solution process as:

$$Stop\ limit = \left|\frac{(UB - LB)}{LB}\right| \tag{12}$$

After satisfying the stop limit, the algorithm will end and the optimal solution of the essential decision variables y is recorded as the output. Otherwise, the number of algorithm iterations will be increased $(k + 1)$, and new constraints will be made and added to the master problem; it will return to step 2.

A summary of the optimization model presented above is indicated in Fig.1. The basic model presented in section (II) Included (1-3) is the unsolvable problem due to uncertainty. To solve, the basic model is separated into two problems by the optimization approach, which includes a master problem including decision variables (4-8) and a sub-problem including uncertain parameters equation(9).

In the first step, the master problem will be solved with zero input equations (4 and 5), in the second step the cutting plates will be applied by equations (6,7 and 8), In the third step, the sub-problem equation (9) will be solved with the results obtained from the master problem. In the fourth step, the convergence boundaries will be updated by equations (10 and 11) by the C&CG method. In the fifth and sixth steps, the convergence conditions of the algorithm will be checked to the specified value. If the stop condition is not met, auxiliary constraints will be created to solve

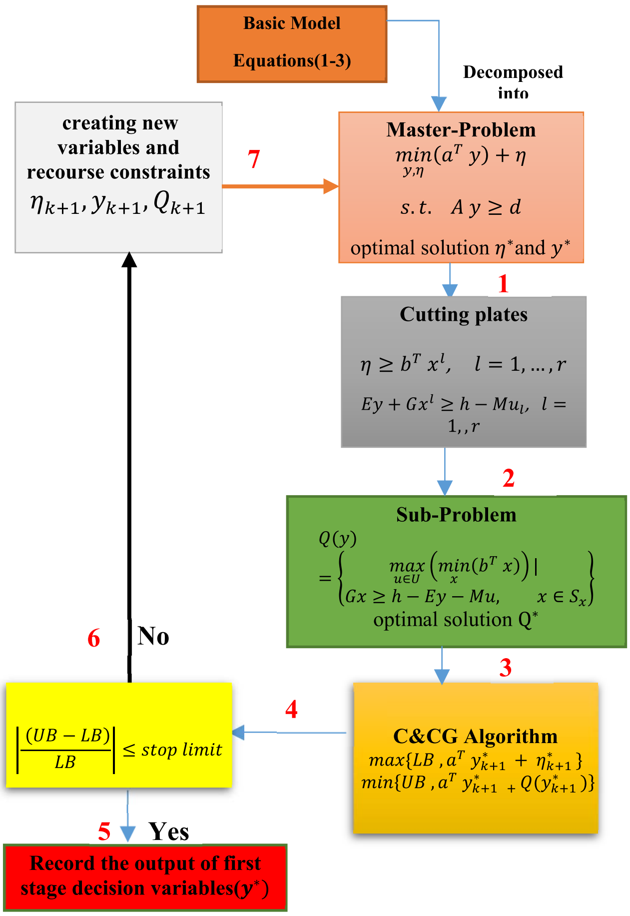

FIGURE 1. Flowchart of the two-stage optimization model.

the master problem in the seventh step and in the second iteration.

III. MODELING UNCERTAINTY SETS

Uncertain parameters in the EMS problem are associated with net inelastic load (d), power purchase and sale prices in the electricity market (λ), and MG islanding event (I). The problem indices, parameters, and decision variables are listed in Tables 22, 23, and 24 respectively see (Appendix A). In this section, the modeling of uncertainty sets for uncertain parameters is presented.

A. MG ISLANDING EVENT UNCERTAINTY SET

The parameter depicting the MG's operation mode is an uncertain binary parameter. When the parameter is 1, it indicates the grid-connected condition and 0 denotes the islanded condition. In this section, we consider that the disturbance in the main grid is observable earlier by using forecast mechanisms and historical data. Determining the time of islanding and duration of the islanding process is highly challenging and has noticeable uncertainty. Similar to the previously considered uncertainty set, an uncertainty budget (Γ^I) is allocated. This budget helps the operator and reduces the challenge of generating the worst scenario by adding the number of additional uncertain hours during the scheduling. Modeling the uncertainty set for islanding events consists of the following terms.

i. For modeling uncertainty sets based on the reliability index of the MG, the uncertain binary parameter is considered to indicate the MG connection status during the full scheduling period (24 hours) based on historic data. To increase the level of conservatism, uncertainty budget (Γ_g) is considered. This parameter limits the number of hours that the MG can become an island. The model presenting the uncertainty set is as following equations.

$$\mathcal{I} := \left\{ I : \sum_{t=1}^{T} (1 - \mathrm{I}_t \le \Gamma_g,\ I_t \in \{0, 1\}, \forall t \right\}; \quad (13)$$

where

$$0 \le \Gamma_g \le T \quad (14)$$

ii. For modeling uncertainty sets based on the resiliency index of the grid, the uncertainty of the parameter is bounded to a certain interval based on the weather forecast.

Therefore, steps of modeling the uncertainty set are considered as following equations:

1) Determine the number of islanding events in a scheduling interval

$$I_1 := \left\{ \boldsymbol{I} : \sum\nolimits_{t \in \Omega_T} (1 - I_t) \le \Gamma^I + \tau, \forall t \in \Omega_T \right\}. \quad (15)$$

2) Determine the interval when the MG is disconnected from the grid

$$I_2 := \left\{ \boldsymbol{I} : I_{t+1} \le I_t, \forall t \in \left[t_1, T^{Isl_1} - 1 \right] \right\}. \quad (16)$$

3) Determine the time intervals based on the weather information that the islanding event occurs as following equation.

$$I_3 := \left\{ \boldsymbol{I} : I_t = 0, \forall t \in \left[T^{Isl_1}, T^{Isl_2} \right] \right\}. \quad (17)$$

4) Determining the time interval of connecting the MG to the grid after fixing the error and stabilizing the conditions until the end of the scheduling interval

$$I_4 := \left\{ \boldsymbol{I} : I_{t-1} \le I_t, \forall t \in \left[T^{Isl_2} + 1, T \right] \right\}. \quad (18)$$

As a result, the model of the considered uncertainty set is obtained from the sharing of relations (15-18).

B. NET INELASTIC LOAD AND ELECTRICITY MARKET PRICES UNCERTAINTY SET

The relation of the uncertainty set considered for the uncertain parameter of the net inelastic load is as following equations.

$$d_{jt} = \bar{d}_{jt} + \hat{d}^+_{jt} \theta^{D+}_{jt} - \hat{d}^-_{jt} \theta^{D-}_{jt}, \quad \forall_j \in \Omega_D,\ t \in \Omega_T \quad (19)$$

where

$$\sum_{t\in\Omega_T}\left(\theta_{jt}^{D+}+\theta_{jt}^{D-}\right)\le\Gamma_j^D,\quad \forall_j\in\Omega_D,\ t\in\Omega_T \tag{20}$$

$$\theta_{jt}^{D+}+\theta_{jt}^{D-}\le 1 \tag{21}$$

$$\left[\bar{d}_{jt}-\hat{d}_{jt}^{-},\bar{d}_{jt}+\hat{d}_{jt}^{+}\right] \tag{22}$$

where the value of the uncertain parameter (net inelastic load) will change as an interval of specified numbers around the nominal value. This interval is as above equation (22), to balance risk and conservatism, the uncertainty budget (Γ) is defined. This uncertainty budget limits the number of hours that the net inelastic load in the intended bus can reach its UB and LB limits. The values of this parameter fall within the $[0, T]$ range. The relation of the uncertainty set considered for the uncertain parameter of electricity market prices is as following equations.

$$\bar{\lambda}_t^{RT}-\hat{\lambda}_t^{RT}\theta_t^{\Lambda-}\le\lambda_t^{RT}\le\bar{\lambda}_t^{RT}+\hat{\lambda}_t^{RT+}\theta_t^{\Lambda+},\quad \forall t\in\Omega_T, \tag{23}$$

where

$$\theta_t^{\Lambda+}+\theta_t^{\Lambda-}\le 1,\quad \forall t\in\Omega_T \tag{24}$$

$$\sum_{t\in\Omega_T}\left(\theta_t^{\Lambda+}+\theta_t^{\Lambda-}\right)\le\Gamma^{\Lambda},\quad t\in\Omega_T, \tag{25}$$

These parameters include the market prices related to positive and negative deviations from the power purchased off the grid and sold to the grid. There is a strong correlation (proximity) between these prices and the actual market price. As a result, instead of defining four separate uncertainty sets a general uncertainty set will be utilized to simplify the computations. Finally, by specifying the value of the uncertainty set and based on the coefficients of these four parameters with the central market price, the powers of all these prices can be obtained separately

$$(\lambda_t^{RT,s-},\lambda_t^{RT,s+},\lambda_t^{RT,b-}\text{ and }\lambda_t^{RT,b+}).$$

The relations between the prices and the main market price are as following equation (26), where vector δ includes known and constant coefficients. The approach to obtaining the uncertainty budget amounts defined in the uncertainty sets is outlined in (Appendix B).

$$\lambda_t^{RT,b+,b-,s+\ and\ s-}=\delta\lambda_t^{RT},\quad \forall t\in\Omega_T. \tag{26}$$

IV. MG EMS MODELLING

A. MG EMS

In this section, the problem of EMS in MGs is modeled in the framework of robust optimization introduced described in section II. First, the objective function and operational constraints of the MG components are written in compact matrix form, and then, the model is mentioned in the framework of the two-stage ARO.

1) 1^{st}-STAGE OBJECTIVE FUNCTION

$$OF_1:\ \sum_{t\in\Omega_T}\sum_{g\in\Omega_{DG}}\left(\lambda_g^{SU}u_{gt}+\lambda_g^{SD}v_{gt}+\alpha_g\chi_{gt}\right)+\sum_{t\in\Omega_T}\left(\lambda_t^{DA,b}P_t^b-\lambda_t^{DA,s}P_t^s\right), \tag{27}$$

where the first stage decision variables includes on/off status of diesel generator, power purchased and sold to the grid in the day-ahead electricity market.

2) 2^d -STAGE OBJECTIVE FUNCTION

$$\begin{aligned}OF_2:\ &\sum_{t\in\Omega_T}\left(\bar{\lambda}_t^{RT,b+}\Delta_t^{b+}+\bar{\lambda}_t^{RT,s-}\Delta_t^{s-}\right)\\ &-\sum_{t\in\Omega_T}\left(\bar{\lambda}_t^{RT,b-}\Delta_t^{b-}+\bar{\lambda}_t^{RT,s+}\Delta_t^{s+}\right)\\ &+\sum_{t\in\Omega_T}\sum_{g\in\Omega_{DG}}\left(\beta_g p_{gt}^{DG}\right)\\ &-\sum_{i\in\Omega_E}\sum_{T_i^a\le t\le T_i^b}\left(\lambda_t^E p_{it}^E\right)\\ &-\sum_{t\in\Omega_T}\sum_{j\in\Omega_D}\left(\lambda_t^d\bar{d}_{jt}\right)\\ &+\sum_{t\in\Omega_T}\sum_{j\in\Omega_D}\left(\lambda_{jt}^{shed}d_{jt}^{shed}\right)\\ &+c_m^{ess}\left(\eta_m^{ch}P_{m,t}^{ch}\Delta t+P_{m,t}^{dch}\Delta t/\eta_m^{dch}\right)\end{aligned} \tag{28}$$

where b^T,λ^T *and* C denote matrices of coefficients of second-stage decision variables, z the second stage decision variables (auxiliary variables) including purchasing/selling power in the real-time electricity market, active power generation in the DGs, supply of elastic/inelastic loads, power losses, and charge/discharge generation capacity of energy storage systems. In this paper, the objective function considered is the type of minimization of operating costs, which in essence seeks to minimize the cost of charge and discharge of energy storage. Since sufficient conditions (e.g., lower charge cost than discharge for maximizing profit) exists the binary variable for avoiding simultaneous charge and discharge of battery can be avoided [34], which improves the speed of convergence of the function to the optimal solution.

3) CONSTRAINTS $Fy\le f$

Where F denotes the matrix of coefficients of first stage decision variables and f is the fixed coefficient matrix. Eqs. (29-35) pertain to the day-ahead electricity market including on/off constraints of the DGs (29-30)

$$x_{g(t-1)}-x_{gt}+u_{gt}\ge 0,\quad \forall_g\in\Omega_{DG},\ t\in\Omega_T; \tag{29}$$

$$x_{gt}-x_{g(t-1)}+v_{gt}\ge 0,\quad \forall_g\in\Omega_{DG},\ t\in\Omega_T; \tag{30}$$

constraints on the minimum time of increasing and decreasing the DGs' power (31-32),

$$x_{gt}-x_{g(t-1)}\ge x_{g\tau},\quad \forall_g\in\Omega_{DG},\ t\in\Omega_T,$$

$$t \neq t_1, \quad \tau \in \left[t+1, \min(t+T_g^U-1, \mathrm{T})\right]; \tag{31}$$

$$x_{g(t-1)} - x_{gt} \geq 1 - x_{g\tau}, \quad \forall_g \in \Omega_{DG}, \ t \in \Omega_T, \quad t \neq t_1, \quad \tau \epsilon \left[t+1, \min(t+T_g^D-1, \mathrm{T})\right]; \tag{32}$$

decomposition of the day-ahead energy scheduling of the MG to positive and negative parts (33),

$$P_t = P_t^b - P_t^s, \quad \forall t \in \Omega_T; \tag{33}$$

constraints on the maximum and minimum energy purchase and sales power in the day-ahead electricity market of the MG (34-35),

$$0 \leq P_t^b \leq S, \quad \forall t \in \Omega_T; \tag{34}$$

$$0 \leq P_t^s \leq S, \quad \forall t \in \Omega_T. \tag{35}$$

4) CONSTRAINTS $H_z \leq h$

Where H denotes the matrix of coefficients of second-stage decision variables, h is fixed coefficient matrix and includes relationships (36-53): constraints on the power increase and decrease rate of the DGs (36),

$$-R_g^D \leq p_{gt}^{DG} - p_{g(t-1)}^{DG} \leq R_g^U, \quad \forall_g \in \Omega_{DG}, \ t \in \Omega_T; \tag{36}$$

modeling the energy storage system (ESS) (37-40),

$$\mathrm{E}_{m,t+1} = \mathrm{E}_{m,t} + \eta_m^{ch} P_{m,t}^{ch} \Delta t - P_{m,t}^{dch} \Delta t / \eta_m^{dch}, \quad \forall_m, t \tag{37}$$

$$0 \leq P_{m,t}^{ch} \leq P_m^{ch,max}, \quad \forall_m, t; \tag{38}$$

$$0 \leq P_{m,t}^{dch} \leq P_m^{dch,max}, \quad \forall_m, t; \tag{39}$$

$$E_m^{min} \leq E_{m,t} \leq E_m^{max}, \quad \forall_m, t; \tag{40}$$

actual power exchanged between the grid and MG (41-43),

$$p_t = p_t^b - p_t^s, \quad \forall \in \Omega_T; \tag{41}$$

$$\Delta_t^b = \Delta_t^{b+} - \Delta_t^{b-}, \quad \forall t \in \Omega_T; \tag{42}$$

$$\Delta_t^s = \Delta_t^{s+} - \Delta_t^{s-}, \quad \forall t \in \Omega_T; \tag{43}$$

constraints on the elastic load (44-45),

$$L_i^E = \sum\nolimits_{t=T_i^a}^{T_i^b} p_{it}^E, \quad \forall_i \in \Omega_E; \tag{44}$$

$$0 \leq P_{it}^E \leq p_i^{E,max}, \quad \forall_i \in \Omega_E, \ t \in \Omega_T, \ T_i^a \leq t \leq T_i^b; \tag{45}$$

AC power flow equations (46-50), where the generation-consumption balance constraint helps the primary control level to secure the dynamic stability of the microgrid.

$$p_t = \sum\nolimits_{n \in \Omega_N} p_{nt}^C, \quad \forall t \in \Omega_T; \tag{46}$$

$$q_t = \sum\nolimits_{n \in \Omega_N} q_{nt}^C, \quad \forall t \in \Omega_T; \tag{47}$$

$$f_{lt}^P = \sum\nolimits_{n:(l,n) \in M_{D_0}} p_{nt}^C, \quad \forall l \in \Omega_L, \ t \in \Omega_T; \tag{48}$$

$$f_{lt}^Q = \sum\nolimits_{n:(l,n) \in M_{D_0}} q_{nt}^C, \quad \forall l \in \Omega_L, \ t \in \Omega_T; \tag{49}$$

The constraint related to the voltage drop of the buses in the AC power flow equations is as follows.

$$\sum_{n:(l,n) \in M_{FT}} v_{nt} - \sum_{n:(l,n) \epsilon M_{t_0}} v_{nt} = \frac{R_l f_{lt}^P + X_l f_{lt}^Q}{V_0}, \quad \forall l \in \Omega_L, \quad t \in \Omega_T; \tag{50}$$

maximum/minimum constraints on the buses' voltage (51),

$$V_n^{min} \leq V_{nt} \leq V_n^{max}, \quad \forall_n \in \Omega_N, \ t \in \Omega_T; \tag{51}$$

maximum active and reactive power passing through the lines (52), and constraints on the maximum re-feeding of the active power in the buses (53),

$$\left(f_{lt}^P\right)^2 + \left(f_{lt}^Q\right)^2 \leq \left(S_l^L\right)^2, \quad \forall l \in \Omega_L, \ t \in \Omega_T; \tag{52}$$

$$0 \leq d_{jt}^{shed} \leq d_{jt}^{shed,max}, \quad \forall_j \in \Omega_D, \ t \in \Omega_T. \tag{53}$$

5) $M_y + N_z \leq w$

Where M matrix of coefficients of first stage decision variables, N matrix of coefficients of second-stage decision variables, w fixed coefficient matrix and includes relationships (54-57): constraints on the active and reactive power generation in the DGs (54-55),

$$p_g^{DG,min} x_{gt} \leq p_{gt}^{DG} \leq p_g^{DG,max} x_{gt}, \quad \forall_g \in \Omega_{DG}, \quad t \in \Omega_T; \tag{54}$$

$$\left(p_{gt}^{DG}\right)^2 + \left(q_{gt}^{DG}\right)^2 \leq \left(S_g^{DG} x_{gt}\right)^2, \quad \forall_g \in \Omega_{DG}, \quad t \in \Omega_T; \tag{55}$$

actual power exchanged between the grid and MG (56-57),

$$\Delta_t^b = p_t^b - P_t^b, \quad \forall t \in \Omega_T; \tag{56}$$

$$\Delta_t^s = p_t^s - P_t^s, \quad \forall t \in \Omega_T. \tag{57}$$

6) CONSTRAINT $K_z \leq I$

Where K denotes the matrix of coefficients of second-stage decision variables, I is the uncertain parameter and includes the following equation,

$$(p_t)^2 + (q_t)^2 \leq \left(S \times \bar{I}_t\right)^2, \quad \forall t \in \Omega_T \tag{58}$$

7) CONSTRAINT $Q_z = d$

Where Q denotes the matrix of coefficients of second-stage decision variables, d uncertain parameter and includes the following equations.

$$p_{nt}^C = \sum\nolimits_{j:(j,n) \in M_D} \left(\bar{d}_{jt} - d_{jt}^{shed}\right) + \sum\nolimits_{i:(i,n) \in M_E} p_{it}^E + \sum\nolimits_{m:(m,n) \in M_{stg}} \left(P_{mt}^{ch} - P_{mt}^{dch}\right) - \sum\nolimits_{g:(g,n) \in M_{DG}} p_{gt}^{DG}, \quad \forall_n \in \Omega_N, \quad t \in \Omega_T; \tag{59}$$

$$q_{nt}^{C} = \sum\nolimits_{j:(j,n)\in M_D}\left(\bar{d}_{jt} - d_{jt}^{shed}\right)\times \tan\left(\varphi_j\right) + \sum\nolimits_{i:(i,n)\epsilon M_E} p_{it}^{E}\times \tan\left(\varphi_i\right) - \sum\nolimits_{g:(g,n)\in M_{DG}} q_{gt}^{DG}, \quad \forall_n \in \Omega_N, \quad t\in\Omega_T \tag{60}$$

B. MIXED-INTEGER LINEAR PROGRAMMING (MILP)

The MG EMS model proposed in the previous section is non-linear due to equations (52), (55), and (58). In other words, to simplify the calculations and accelerate the problem-solving process, an appropriate linear approximation approach is adopted. This approach is inspired by Euclidean ball [35]. The linearization equation and its equivalent equations are as following equations:

$$r_1^2 + r_2^2 \le r^2 \tag{61}$$

The above second-order equation can be linearized by using the following three equations.

$$-\sqrt{3}\left(r_1 + kr\right) \le r_2 \le -\sqrt{3}\left(r_1 - kr\right) \tag{62}$$

$$-\frac{\sqrt{3}}{2}kr \le r_2 \le \frac{\sqrt{3}}{2}kr \tag{63}$$

$$\sqrt{3}\left(r_1 - kr\right) \le r_2 \le \sqrt{3}\left(r_1 + kr\right) \tag{64}$$

Here, k is the linearization coefficient. The error resulting from the approximations can be reduced by increasing the number of unequal linear relations.

C. MG EMS IN TWO-STAGE ARO FRAMEWORK

The framework of the two-stage ARO model is given by following equations

$$\min_{y}\left(a^T y\right) + \max_{d,\lambda,I}\left(\min_{z\in Z(y,d,\lambda,I)}\left(b_z^T + \lambda^T C_z + e^T d\right)\right) \tag{65}$$

$$s.t.\ F_y \le f \tag{66}$$

$$Z\left(y,d,\lambda,I\right) = \left\{z: H_z \le h, M_y + N_z \le w, K_z \le I, Q_z = d\right\} \tag{67}$$

This model is a complex model that can not be solved using existing software. By breaking it down into the master problem and sub-problem it becomes computationally tractable.

1) SUB-PROBLEM

The innermost maximum-minimum problem is a linear model and, therefore, has strong duality. Therefore, the dual problem is presented as the following equations. The dual calculation process of Equations (65-67) is described in (Appendix C).

$$R\left(y,d,\lambda,I\right) = \max_{\pi\varsigma,\vartheta,\rho}\left(\varsigma^T M_y + e^T d - \pi^T h - \varsigma^T w - \vartheta^T I - \rho^T d\right) \tag{68}$$

$$s.t.\ \pi^T H + \varsigma^T N + \vartheta^T K + \lambda^T C + \rho^T Q + b^T = 0 \tag{69}$$

$$\forall_\pi \ge 0, \quad \varsigma \ge 0, \ \vartheta \ge 0, \ \rho\ free \tag{70}$$

where ϑ, π, ρ, and ς present the problem variables. The obtained dual equation which is of the maximum type can be combined with the previous maximum problem. As a result, the objective function and the constraint obtained for the sub-problem are in the form of equations (71-73) relations.

$$X\left(y\right) = \max_{\pi,\varsigma,\vartheta,\rho,d,\lambda,I}\left(\varsigma^T M_y + e^T d - \pi^T h - \varsigma^T w - \vartheta^T I - \rho^T d\right) \tag{71}$$

$$s.t.\ \pi^T H + \varsigma^T N + \vartheta^T K + \lambda^T C + \rho^T Q + b^T = \mathbf{0} \tag{72}$$

$$\forall_{\boldsymbol{\pi}} \ge 0, \quad \boldsymbol{\varsigma} \ge 0, \ \boldsymbol{\vartheta} \ge 0, \ \boldsymbol{\rho}\ free, \ \boldsymbol{d}\in D, \ \boldsymbol{\lambda}\epsilon\Lambda, \ \boldsymbol{I}\in I \tag{73}$$

The sub-problem is nonlinear due to the multiplication of a binary parameter in a continuous variable ($\vartheta^T I$ and $\rho^T d$). The big-M linearization method (see Appendix D) is used.

2) MASTER PROBLEM

The objective function of the problem is of the minimum type. In the following equations, is the vector of recourse variables related to scenario (s) also all the scenarios are executable. The master problem is modeled as following equations,

$$\min_{y,\psi,z_s}\left(a^T y\right) + \psi \tag{74}$$

$$F_y \le f \tag{75}$$

$$\psi \ge b^T z_s + \lambda_s^T C_z + e^T d_s, \quad \forall_s \in \mathcal{G} \tag{76}$$

$$Hz_s \le h, \quad \forall_s \in \mathcal{G} \tag{77}$$

$$M_y + N_{z_s} \le w, \quad \forall_s \in \mathcal{G} \tag{78}$$

$$Kz_s \le I_s, \quad \forall_s \in \mathcal{G} \tag{79}$$

$$Qz_s = d_s, \quad \forall_s \in \mathcal{G} \tag{80}$$

The optimal solutions of the problem are obtained at extreme points by multiplying the members of the three uncertainty sets. Accordingly, the number of solutions, or the number of existing scenarios, is a finite and countable value. The set of scenarios is as following equation,

$$\left(s \in \mathcal{G} = \left\{s_1, s_2, \ldots, s_N\right\}\right) \tag{81}$$

As a result, the problem of EMS can be solved by using the C&CG algorithm.

D. SUMMARY OF PRE-PERTURBATION SCHEDULING IN THE MG

A summary of the pre-perturbation scheduling scheme in MGs is shown in Fig. 2. The first step is to determine the uncertainty sets based on historical and predicted data. At this stage, the MG operator must identify the uncertainty budgets with the introduced approach. Once the uncertainty sets are identified, the next step includes a proposed scheduling scheme that solves the problem using the C&CG algorithm. In each iteration, auxiliary variables (second stage variables) are created and added to the first stage, and this process will

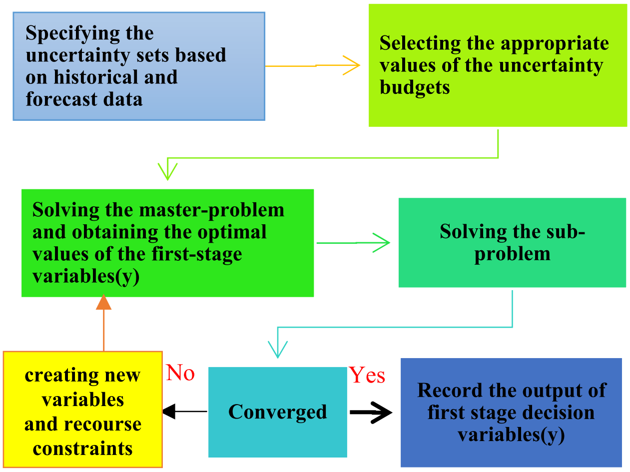

FIGURE 2. Outline of the proposed scheme for the pre-perturbation scheduling in the MG.

TABLE 1. Technical data of the DG unit.

Unit	P^{DGmin}	P^{DGmax}	S^{DG}	T^U	T^D	R^U	R^D	λ^{SU}	λ^{SD}
DG	1	4.2	4.2	2	2	144	144	15	10

TABLE 2. Technical data of the ESS.

Unit	E^{min}	E^{max}	P^{chmax}	P^{dchmax}
Storage	0.5	4.75	1	1

TABLE 3. Parameters.

Parameters	Values	Parameters	Values
α_g	79	V°	1
β_g	27	S	5
$\eta_m^{ch/dch}$	0.95	Δ_t	1
c^{ess}	65	T	6
V^{min}	0.95	T^{Isl_1}	3
V^{max}	1.05	T^{Isl_2}	3

continue until the stop criterion is reached. As a result, the optimal values of the first-stage variables (y) are obtained.

V. NUMERICAL RESULTS

All the numerical tests are performed on a personal computer with a core i5@1.60 GHz and 4 GB RAM. The C&CG algorithm and the MILP master and recourse problems were solved with IBM ILOG CPLEX 12.4 solver [36].

A. THE STUDIED SYSTEM DESCRIPTION

The components of this MG include inelastic loads, elastic loads, RES, DG, ESS, distribution transformer, and the main grid. The numerical data for the DG, ESS, parameters, day-ahead electricity market price chart, and elastic load is given in Tables 1, 2, and 3 and Figs. 3 and 4, respectively. The MG structure is presented in Fig. 5. The scheduling period includes four 6-hour intervals. One-hour scheduling interval

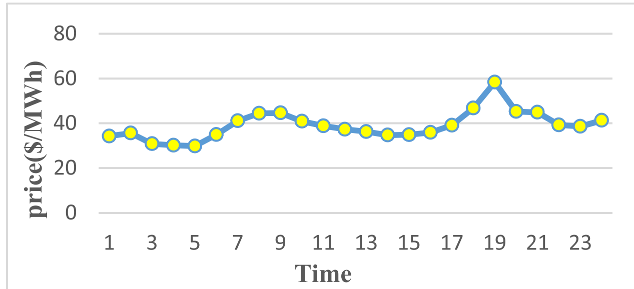

FIGURE 3. Day-ahead market electricity price.

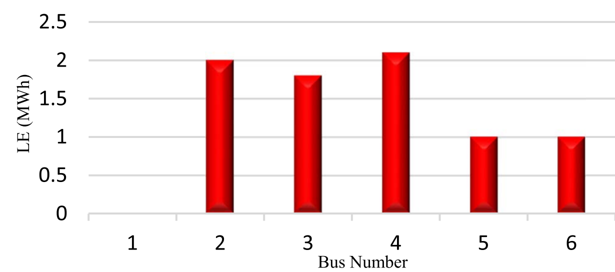

FIGURE 4. Elastic energy load.

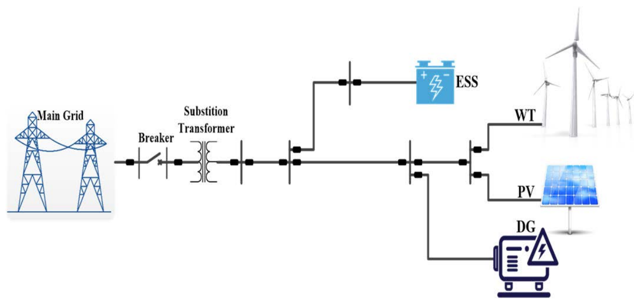

FIGURE 5. MG structure.

and uncertain inelastic load are placed in bus 4. Uncertainty is considered for the uncertain inelastic load, and the actual market cost coefficient is assumed to be 30%. The duration of using elastic loads is as the following vectors:

$$T^a(i) = \begin{bmatrix} i_1 & 1. & i_2 & 1. & i_3 & 2. & i_4 & 2. & i_5 & 3 \end{bmatrix};$$
$$T^b(i) = \begin{bmatrix} i_1 & 5. & i_2 & 5. & i_3 & 6. & i_4 & 6. & i_5 & 6 \end{bmatrix}.$$

B. SIMULATION RESULTS

Several scenarios are tested to assess the effectiveness of the proposed method in finding the optimal solution. The problem is solved by considering one uncertain parameter (net inelastic load), two uncertain parameters (net inelastic load and electricity market price), and then three uncertain parameters. The final report includes the results of three uncertain parameters scenarios with different uncertainty budgets in the first scheduling period as well as the results of other scheduling periods. First, we discuss the process of reaching the result for optimal output of the first stage decision variables, uncertain parameters, and the optimal stop limit for the algorithm, for the first scheduling interval (IV-XIX). The results of all scheduling intervals are in the form of table 20 and Figs. 6 to 8. Figure 9 shows the comparison between the C&CG and Benders algorithms for all scheduling intervals.

The simulated scenarios are as follows: Simulation results of net inelastic load with budget 5 (scenario A); net inelastic load with budget 6 (scenario B); net inelastic load and electricity market price with budget 5 (scenario C); net inelastic load and electricity market price with budget 6 (scenario D); net inelastic load and electricity market price with budget 6 and islanding with budget 0 (scenario E); net inelastic load and electricity market price with budget 6 and islanding with budget 1 (scenario F); net inelastic load and the electricity market price with budget 6 and islanding with budget 2 (scenario G); second period (electricity market price and net inelastic load) with uncertainty budget 5 (scenario H); third period (electricity market price and net inelastic load) with uncertainty budget 5 (scenario I) and fourth period (electricity market price and net inelastic load) with uncertainty budget 6 (scenario J).

TABLE 4. The first iteration for one uncertain parameter with budget5.

variables	t_1	t_2	t_3	t_4	t_5	t_6
P^{Buy}	0	0	0	0	0	0
P^{Sell}	5	5	5	5	5	5
x_g	0	0	0	0	0	0
d_3	0.12	0.156	0.156	0.156	0.156	0.12

In the first iteration, the optimal solution of the decision variables (on/off status of the DG (x), power exchanged with the grid in the day-ahead market (p)), and the optimal value of the uncertain parameter of net inelastic load (d) are given in table (4). In the first iteration, the microgrid is in the mode of selling power to the main grid and off DG during the scheduling period. The algorithm stop condition is calculated in table (5):

TABLE 5. Stop limit in the first iteration for one uncertain parameter.

	LB	UB	Stop limit
First iteration	-293.31	776.302	3.65

Based on the result of the stop limit of the C&CG algorithm (table 5), in the first iteration, the algorithm stop condition (stop limit ≤ 0.005) is not met; therefore, it enters the second iteration with new auxiliary variables. The second iteration of the algorithm is given in table (6):

Based on table 6, the DG is on at 5:00 and 6:00, and at 6:00, the microgrid has purchased 0.11 (MW) of power from the grid. Then, the algorithm stop limit is examined in table 7.

In this iteration, the algorithm stop limit (stop limit $\leq$ 0.005) is met and the solution process stops.

TABLE 6. The second iteration for one uncertain parameter with budget5.

variables	t_1	t_2	t_3	t_4	t_5	t_6
P^{Buy}	0	0	0	0	0	0.11
P^{Sell}	0	0	0	0	0	0
x_g	0	0	0	0	1	1
d_3	0.156	0.156	0.156	0.12	0.156	0.156

TABLE 7. Stop limit in the second iteration of uncertain parameter with budget 5.

	LB	UB	Stop limit	operational cost
Second iteration	777.008	776.302	0.0009	176.837

TABLE 8. The optimal state of decision variables and uncertain parameters in scenario B.

variables	t_1	t_2	t_3	t_4	t_5	t_6
P^{Buy}	0	0	0	0	0	0
P^{Sell}	5	5	5	5	5	5
x_g	0	0	0	0	0	0
d_3	0.156	0.156	0.156	0.156	0.156	0.156
λ^{RT}	-	-	-	-	-	-
I	-	-	-	-	-	-

In the optimal solution, the microgrid is in the mode of selling power to the main grid and off DG during the scheduling period. The algorithm stop condition is calculated in table 9.

TABLE 9. Stop limit and optimal boundaries in scenario B.

LB	UB	operational cost	Stop limit
796.386	795.754	176.837	0.0007

The algorithm stop limit (stop limit $\leq$ 0.005) is met and the solution process stops.

In the optimal solution, the microgrid is in the mode of selling power to the main grid and the diesel generator is on at 5 and 6 o'clock during the scheduling period. The optimal values of the uncertain parameters of net inelastic load(d) and electricity market prices(λ) during the scheduling period are based on the above table. Net inelastic load in 5 hours and electricity market price in 2 hours have changed from the nominal values.

The algorithm stop limit (stop limit $\leq$ 0.005) is met and the solution process stops.

In the optimal solution, the microgrid is in the mode of selling power to the main grid and off DG during the scheduling period. The optimal values of the uncertain parameters of net inelastic load (d) and electricity market prices(λ)during the scheduling period are based on the table above. Net inelastic

TABLE 10. The optimal state of decision variables and uncertain parameters in scenario C.

variables	t_1	t_2	t_3	t_4	t_5	t_6
P^{Buy}	0	0	0	0	0	0
P^{Sell}	5	5	5	5	5	5
x_g	0	0	0	0	1	1
d_3	0.156	0.156	0.156	0.12	0.156	0.156
λ^{RT}	34.248	24.928	30.83	21.105	29.8	34.9
I	-	-	-	-	-	-

TABLE 11. Stop limit and optimal boundaries in scenario C.

LB	UB	operational cost	Stop limit
784.645	787.359	176.838	0.0034

TABLE 12. The optimal state of decision variables and uncertain parameters in scenario D.

variables	t_1	t_2	t_3	t_4	t_5	t_6
P^{Buy}	0	0	0	0	0	0
P^{Sell}	5	5	5	5	5	5
x_g	0	0	0	0	0	0
d_3	0.155	0.155	0.155	0.155	0.155	0.155
λ^{RT}	34.248	24.928	30.83	30.15	29.8	24.43
I	-	-	-	-	-	-

TABLE 13. Stop limit and optimal boundaries in scenario D.

LB	UB	operational cost	Stop limit
794.438	796.715	173	0.0028

load in 6 hours and electricity market price in 2 hours have changed from the nominal values.

The algorithm stop limit (stop limit $\leq$ 0.005) is met and the solution process stops.

Based on table 14, the DG is off during the scheduling hours and, in six hours, the microgrid sells the power of 5 (MW) to the grid. The uncertain parameter (d) in six hours and the electricity market prices in two hours change from their nominal values. The connection of the microgrid (I) is stopped at 3:00 and it is islanded.

The algorithm stop limit (stop limit $\leq$ 0.005) is met and the solution process stops.

Based on table 16, the DG is off during the scheduling hours and, in six hours, the microgrid sells the power of 5 (MW) to the grid. The uncertain parameter (d) in six hours and the electricity market prices in two hours change from their nominal values. The connection of the microgrid (I) is stopped at 3:00, 4:00 and it is islanded.

TABLE 14. The optimal state of decision variables and uncertain parameters in scenario E.

variables	t_1	t_2	t_3	t_4	t_5	t_6
P^{Buy}	0	0	0	0	0	0
P^{Sell}	5	5	5	5	5	5
x_g	0	0	0	0	0	0
d_3	0.155	0.155	0.155	0.155	0.154	0.121
λ^{RT}	34.248	24.928	30.83	30.15	20.86	34.9
I	1	1	0	1	1	1

TABLE 15. Stop limit and optimal boundaries in scenario E.

LB	UB	operational cost	Stop limit
808.53	806.773	173	0.0021

TABLE 16. The optimal state of decision variables and uncertain parameters in scenario F.

variables	t_1	t_2	t_3	t_4	t_5	t_6
P^{Buy}	0	0	0	0	0	0
P^{Sell}	5	5	5	5	5	5
x_g	0	0	0	0	0	0
d_3	0.153	0.154	0.154	0.153	0.154	0.154
λ^{RT}	23.974	24.928	30.83	30.15	29.8	34.9
I	1	1	0	0	1	1

TABLE 17. Stop limit and optimal boundaries in scenario F.

LB	UB	operational cost	Stop limit
829.218	831.88	173	0.0032

TABLE 18. The optimal state of decision variables and uncertain parameters in scenario G.

variables	t_1	t_2	t_3	t_4	t_5	t_6
P^{Buy}	0	0	0	0	0	0
P^{Sell}	5	5	5	5	5	5
x_g	0	0	0	0	0	0
d_3	0.153	0.154	0.154	0.153	0.154	0.154
λ^{RT}	23.974	24.928	30.83	30.15	29.8	34.9
I	1	1	0	0	0	1

The algorithm stop limit (stop limit $\leq$ 0.005) is met and the solution process stops.

Based on table 18, the DG is off during the scheduling hours and, in six hours, the microgrid sells the power of 5 (MW) to the grid. The uncertain parameter (d) in six hours and the electricity market prices in two hours change

TABLE 19. Stop limit and optimal boundaries in scenario G.

LB	UB	operational cost	Stop limit
834.378	831.88	173	0.0029

TABLE 20. Simulation results of all scheduling intervals.

scenario	variables	t_1	t_2	t_3	t_4	t_5	t_6	LB	UP
E	P^{Buy}	0	0	0	0	0	0	808.53	806.773
	P^{Sell}	5	5	5	5	5	5		
	x_g	0	0	0	0	0	0		
	p^{ch}	0	0	0	0	0	0		
	p^{dch}	0	0	0	0	0	0.475		
H	P^{Buy}	0	0	0	0	0.11	0	953.15	953.714
	P^{Sell}	0	0	0	0	0	0		
	x_g	0	0	0	0	1	1		
	p^{ch}	0	0	0	0	0	0		
	p^{dch}	0	0	0	0	0	0.475		
I	P^{Buy}	0	0	0	0	0	0	840.25	837.6
	P^{Sell}	0	0	0	0	0	0		
	x_g	0	0	0	0	1	1		
	p^{ch}	0	0	0	0	0	0		
	p^{dch}	0	0	0	0	0	0.475		
J	P^{Buy}	0	0	0	0	0	0	986.34	984.081
	P^{Sell}	0	0	0	0	0	0		
	x_g	1	1	0	0	0	0		
	p^{ch}	0	0	0	0	0	0		
	p^{dch}	0.288	0	0	0	0	0.475		

from their nominal values. The connection of the microgrid (I) is stopped at 3:00, 4:00 and 5:00 and it is islanded.

The results of the uncertain parameters obtained for the second to fourth scheduling intervals are in the form of Figures 6-8.

Fig.9. shows the advantages of the C&CG method compared to the Benders algorithm, which includes fewer iterations and shorter solving times to achieve the optimal solution. According to this fig 9(a), where the C&CG algorithm reaches the optimal solution after 29.45 (s) and 115 (s) for the Benders algorithm. Another comparison is the iteration numbers that takes to reach the optimal solution figure 9(b), for scenario (E) the C&CG algorithm reaches the optimal solution in 2 iterations, but the Benders algorithm reaches the optimal solution in 21 iterations. In both algorithms, the value of the obtained objective function is the same. The comparison results between the two algorithms for the other scenarios are shown in the figure.

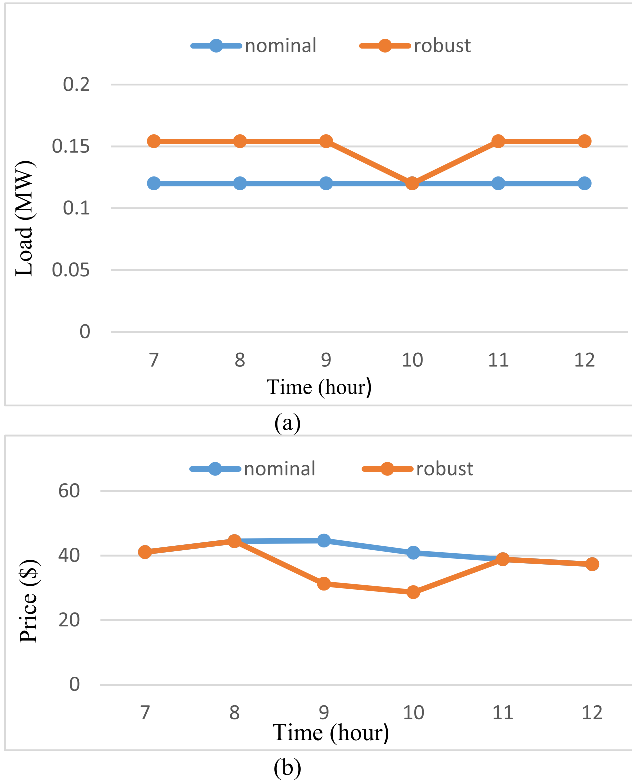

FIGURE 6. Uncertain parameters obtained in the second time interval: (a) Net inelastic load values; (b) Electricity market price values.

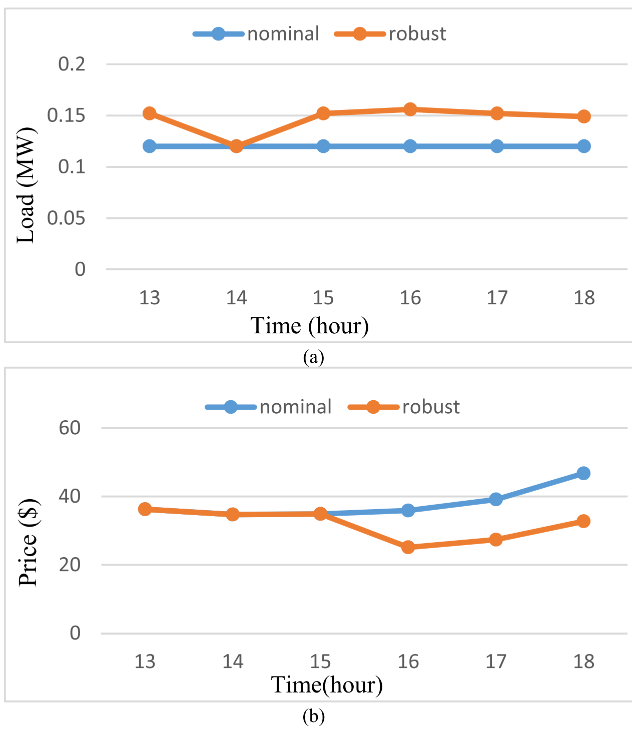

FIGURE 7. Uncertain parameters obtained in the third time interval: (a) Net inelastic load values; (b) Electricity market price values.

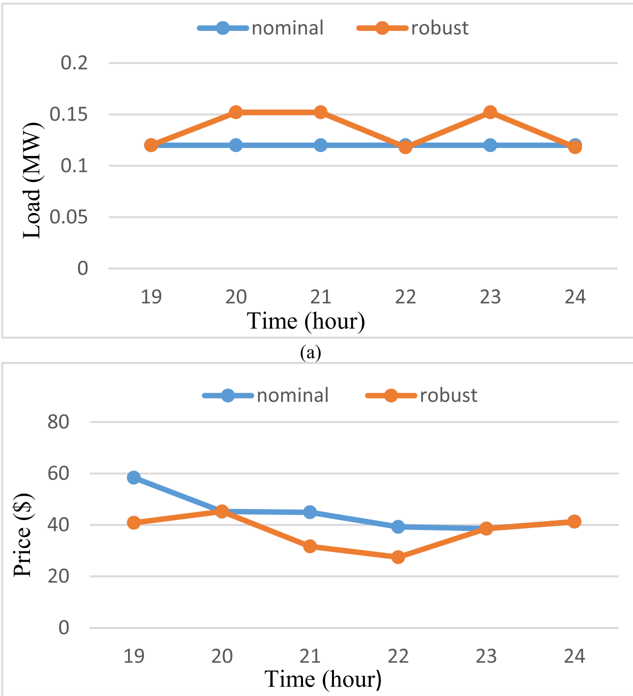

FIGURE 8. Uncertain parameters obtained in the fourth time interval: (a) Net inelastic load values; (b) Electricity market price values.

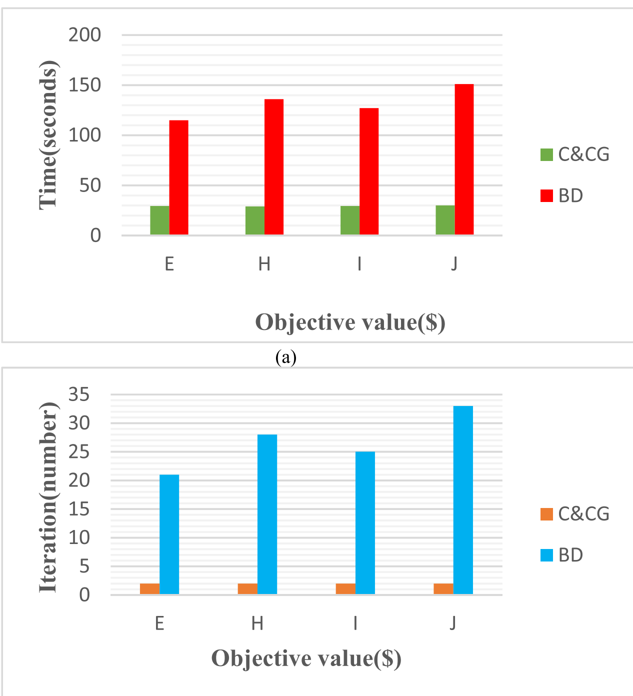

FIGURE 9. Comparison between C&CG and Benders algorithms: (a) Solution Time(seconds); (b) Iteration.

C. FINAL REPORT

The final result of the considered scenarios is shown in Table 21. In the first scheduling interval, it is assumed that an islanding event has occurred and that all three uncertain parameters have values. The criterion for selecting each scenario is the minimum value of the objective function and the operating cost.

TABLE 21. The final results of the simulated scenarios.

scenario	Z
E	808.53$
H	953.152$
I	840.251$
J	986.34$

VI. CONCLUSION

In this paper, pre-perturbation scheduling in MGs was proposed to minimize operational costs and the damaging outcomes of islanding events. The optimal scheduling mode of the DGs and the optimal energy exchange in the day-ahead market were obtained with an two-stage adaptive ARO and by using the C&CG algorithm. First, this framework was formulated as a MILP problem; then, to create a practical approach for large-scale MGs, it was decomposed into a master problem and a solvable sub-problem.

Based on the results obtained in the simulation section, the general results of this paper can be written as follows:

1) Using the C&CG algorithm, rapid convergence of the optimal solution was achieved. The number of iterations of the model solution in the C&CG has been reduced compared to the Benders algorithm for the first scheduling interval 21 to 2, the second interval 28 to 2, the third interval 25 to 2, and the fourth time period 33 to 2 number reduced.
2) Modeling the uncertainty associated with the MG islanding events due to resiliency-oriented indexes based on weather information in a scheduling period reduced operating costs. For the first period from 834.378$ to 808.53$, the second period from 953.248$ to 953.152$, the third period from 852.868$ to 840.251$, and the fourth period from 986.34$ to 964.982$ reduced.
3) Using the C&CG algorithm and appropriately selecting the number of uncertainty budgets and quantitative examination of their impact on the optimal solution reduced the time complexity of the solution. Problem-solving time by the C&CG algorithm has been reduced compared to the Benders algorithm for the first scheduling interval 115 to 29.45 seconds, the second interval 136 to 29 seconds, the third interval 127 to 29.5 seconds, and the fourth time period 151 to 30 seconds reduced.

APPENDIX A

See Tables 22–24.

APPENDIX B UNCERTAINTY BUDGET

By determining a proper uncertainty budget, a robust solution will have higher economic efficiency than the stochastic

TABLE 22. List of indices, sets, and symbols.

g	Diesel generator index
i/j	Elastic/inelastic load index
m	Energy storage system index
L/n	Line / node index
k	Repetition index
t	Time index
$\Omega_{E/D}$	Elastic/inelastic load set
Ω_{DG}	Diesel generator set
$\Omega_{L/n}$	Load / node set
Ω_{stg}	Energy storage system set
Ω_T	Time set
M_{DG}	Diesel generators location map
M_{DS}	Map of connecting lines between nodes
M_{stg}	Energy storage system location map
$M_{Fr/To}$	Map of lines entering/exiting nodes
$M_{E/D}$	Map of the location of elastic/inelastic loads
$(\bar{0}), (\hat{0})^{+/-}$	The nominal value, upper/lower limit of parameters
$(0)^*$	Indicates the optimal value of the variables
$(0)^{max/min}$	Indicates the value of max/min variables

TABLE 23. List of parameters.

Parameter	Details	Units
α, β	Cost coefficients of diesel generators	\$
d	Uncertain load consumption parameter	MW
I	The binary parameter indicates the status of the MG	0/1
L^E	Consumable elastic load	MW
R/x	Resistance/reactance of line	Ω
$R^{U/D}$	Increase/decrease power of diesel generators	-
$S/S^{DG/SL}$	Appearance of transformer / diesel generator / lines	-
$T^{U/D}$	Increase/decrease power of diesel generators	-
λ^{shed}	Consumption cost	\$
$\lambda^{SU/SD}$	Cost of turning on / off diesel generators	\$
φ	The angle between current and voltage loads	degree
Γ	Uncertainty budget	-
c^{ess}	Energy storage system cost factor	\$
$\eta_m^{ch/dch}$	Charging/discharging efficiency of energy storage system	-
Δt	Length of scheduling courses	-
$\lambda^{DA,b/s}$	The cost of buying/selling in the day-ahead market	\$
$\lambda^{RT,b+/-}$	Real-time market cost ratio	\$
$\lambda^{RT,s+/-}$	Real-time market cost ratio	\$
$\lambda^{E/d}$	Cost ratio of elastic/inelastic load supply	\$

approach. Based on the boundary defined in the following equation, the uncertainty budget can be determined with each level of probability. In the following equations, n is the number of random variables in the equation, and $\Phi(x)$ is a function of the cumulative distribution. By considering 95% probability and six random variables, the budget of uncertainty 5 and 6 is obtained [37]. The resulting budgets are also used for real-time electricity market price uncertainty.

$$\Gamma_j^D \geq \Phi^{-1}(0.95)\sqrt{n} \tag{82}$$

APPENDIX C DUAL PROBLEM

The internal minimum function and its constraint are as follows.

$$\min_{z\in Z(y,d,\lambda,I)} \left(b_z^T + \lambda^T C_z + e^T d\right) \tag{83}$$

$$Z(y,d,\lambda,I) = \left\{z : H_z \leq h, M_y + N_z \leq w, K_z \leq I, Q_z = d\right\} \tag{84}$$

TABLE 24. List of variables.

Variables	Details	Units
d^{shed}	Feed reload	MW
V	Node voltage	P.U
X	Scheduling status of diesel generators	0/1
E	Energy level of energy storage systems	MW
$f^{P/Q}$	Active/reactive power of lines	MW
$p^{b/s}$	Buy/sell power in the microgrid in the day-ahead market	MW
p^E	Elastic load active power	MW
u/v	Scheduling status of diesel generators	0/1
p^{DG}/q^{DG}	Active/reactive power of diesel generators	MW
p^c/q^c	Active/reactive power of nodes	MW
θ	A binary variable used in uncertainty set	0/1
p^{ch}/p^{dch}	Charging / discharging power of energy storage system	MW
$\Delta^b, \Delta^{b+/-}$	Total and positive/negative differences between P^b and p^b	-
$\Delta^s, \Delta^{s+/-}$	Total and positive/negative differences between P^s and p^s	-
q	Real-time reactive power exchanged with the grid	MW
P/p	Scheduled/real-time power exchanged grid	MW
$p^{b/s}$	Real-time active power bought/sold with grid	MW

To obtain the duality of (83), since the objective function is of the minimum type, all constraints must be written as ($\geq \mathbf{0}$).

$$\min_{z\in Z(y,d,\lambda,I)} \left(b_z^T + \lambda^T C_z + e^T d\right) \tag{85}$$

$$-H_z \geq -h \tag{86}$$

$$-N_z \geq M_y - w \tag{87}$$

$$-K_z \geq -I \tag{88}$$

$$Q_z \geq d \tag{89}$$

$$-Q_z \geq -d \tag{90}$$

By considering the dual variables that include (ϑ, π, ρ, and ς) and multiplying by the above constraints, the dual function of the maximum type can be obtained.

$$R(y,d,\lambda,I) = \max_{\pi\,\varsigma,\vartheta,\rho} \left(\varsigma^T M_y + e^T d - \pi^T h - \varsigma^T w - \vartheta^T I - \rho^T d\right) \tag{91}$$

$$s.t.\ \pi^T H + \varsigma^T N + \vartheta^T K + \lambda^T C + \rho^T Q + b^T = 0 \tag{92}$$

$$\forall_\pi \geq 0, \quad \varsigma \geq 0, \vartheta \geq 0, \ \rho free \tag{93}$$

APPENDIX D BIG-M METHOD

The non-linear terms in equation (71) include $\rho^T d$ and $\vartheta^T I$. The defined recourse continuous variables are given as following equation

$$\rho_{nt}\theta_{jt}^{D+} = \sigma_{nt}^+, \quad \rho_{nt}\theta_{jt}^{D-} = \sigma_{nt}^- \ and\ \xi_t \triangleq \vartheta_t I_t \tag{94}$$

The general relation of the inelastic load is given as the following equation

$$d_{jt} = \bar{d}_{jt} + \hat{d}_{jt}^+\theta_{jt}^{D+} - \hat{d}_{jt}^-\theta_{jt}^{D-}, \quad \forall_j \in \Omega_D,\ t \in \Omega_T \tag{95}$$

By applying the following equations (96-101), the recourse innermost maximum-minimum problem is converted into a

MILP problem.

$$-M^I I_t \leq \xi_t \leq M^I I_t, \quad \forall_t \in \Omega_T \tag{96}$$

$$-M^I (1 - I_t) \leq \xi_t - \vartheta_t \leq M^I (1 - I_t), \quad \forall_t \in \Omega_T \tag{97}$$

$$-M^{\theta +}\theta_{jt}^{D+} \leq \sigma_{nt}^{+} \leq M^{\theta +}\theta_{jt}^{D+}, \quad \forall_n \in \Omega_T, \quad t \in \Omega_T,\ j:(j,n) \in M_D \tag{98}$$

$$-M^{\theta +}\left(1 - \theta_{jt}^{D+}\right) \leq \sigma_{nt}^{+} - \rho_{nt} \leq M^{\theta +}(1 - \theta_{jt}^{D+}), \quad \forall_n \in \Omega_T, \quad t \in \Omega_T,\ j:(j,n) \in M_D \tag{99}$$

$$-M^{\theta -}\theta_{jt}^{D-} \leq \sigma_{nt}^{-} \leq M^{\theta -}\theta_{jt}^{D-}, \quad \forall_n \in \Omega_T, \quad t \in \Omega_T,\ j:(j,n) \in M_D \tag{100}$$

$$-M^{\theta -}\left(1 - \theta_{jt}^{D-}\right) \leq \sigma_{nt}^{-} - \rho_{nt} \leq M^{\theta -}(1 - \theta_{jt}^{D-}), \quad \forall_n \in \Omega_T, \quad t \in \Omega_T,\ j:(j,n) \in M_D \tag{101}$$

REFERENCES

[1] M. H. Moradi, M. Eskandari, and H. Showkati, "A hybrid method for simultaneous optimization of DG capacity and operational strategy in microgrids utilizing renewable energy resources," *Int. J. Electr. Power Energy Syst.*, vol. 56, pp. 241–258, Mar. 2014.

[2] M. H. Moradi, M. Eskandari, and S. M. Hosseinian, "Cooperative control strategy of energy storage systems and micro sources for stabilizing microgrids in different operation modes," *Int. J. Elect. Power Energy Syst.*, vol. 78, pp. 390–400, Jun. 2016.

[3] L. Che, M. Khodayar, and M. Shahidehpour, "Only connect: Microgrids for distribution system restoration," *IEEE Power Energy Mag.*, vol. 12, no. 1, pp. 70–81, Jan./Feb. 2014.

[4] W.-J. Ma, J. Wang, V. Gupta, and C. Chen, "Distributed energy management for networked microgrids using online ADMM with regret," *IEEE Trans. Smart Grid*, vol. 9, no. 2, pp. 847–856, Mar. 2018.

[5] C. Zhang, Y. Xu, Z. Y. Dong, and K. P. Wong, "Robust coordination of distributed generation and price-based demand response in microgrids," *IEEE Trans. Smart Grid*, vol. 9, no. 5, pp. 4236–4247, Sep. 2018.

[6] Y. Guo and C. Zhao, "Islanding-aware robust energy management for microgrids," *IEEE Trans. Smart Grid*, vol. 9, no. 2, pp. 1301–1309, Mar. 2018.

[7] T. Shekari, S. Golshannavaz, and F. Aminifar, "Techno-economic collaboration of PEV fleets in energy management of microgrids," *IEEE Trans. Power Syst.*, vol. 32, no. 5, pp. 3833–3841, Sep. 2017.

[8] M. H. Moradi and M. Eskandari, "A hybrid method for simultaneous optimization of DG capacity and operational strategy in microgrids considering uncertainty in electricity price forecasting," *Renew. Energy*, vol. 68, pp. 697–714, Aug. 2014.

[9] J. Chen, W. Zhang, J. Li, W. Zhang, Y. Liu, B. Zhao, and Y. Zhang, "Optimal sizing for grid-tied microgrids with consideration of joint optimization of planning and operation," *IEEE Trans. Sustain. Energy*, vol. 9, no. 1, pp. 237–248, Jan. 2018.

[10] A. Askarzadeh, "A memory-based genetic algorithm for optimization of power generation in a microgrid," *IEEE Trans. Sustain. Energy*, vol. 9, no. 3, pp. 1081–1089, Jul. 2018.

[11] H. Farzin, M. Fotuhi-Firuzabad, and M. Moeini-Aghtaie, "A stochastic multi-objective framework for optimal scheduling of energy storage systems in microgrids," *IEEE Trans. Smart Grid*, vol. 8, no. 1, pp. 117–127, Jan. 2017.

[12] J. S. Giraldo, J. A. Castrillon, J. C. Lopez, M. J. Rider, and C. A. Castro, "Microgrids energy management using robust convex programming," *IEEE Trans. Smart Grid*, vol. 10, no. 4, pp. 4520–4530, Jul. 2019.

[13] Y. Fu, Z. Zhang, Z. Li, and Y. Mi, "Energy management for hybrid AC/DC distribution system with microgrid clusters using non-cooperative game theory and robust optimization," *IEEE Trans. Smart Grid*, vol. 11, no. 2, pp. 1510–1525, Mar. 2020.

[14] E. Mokaramian, H. Shayeghi, F. Sedaghati, A. Safari, and H. H. Alhelou, "An optimal energy hub management integrated EVs and RES based on three-stage model considering various uncertainties," *IEEE Access*, vol. 10, pp. 17349–17365, 2022.

[15] M. H. Moradi, M. Eskandari, and S. M. Hosseinian, "Operational strategy optimization in an optimal sized smart microgrid," *IEEE Trans. Smart Grid*, vol. 6, no. 3, pp. 1087–1095, May 2015.

[16] X. Zeng, H. Wu, M. Ding, R. Bi, B. Xu, and J. Ding, "Two-stage robust optimization for practical reactive power in distribution network based on multiple constraint convex approximation," *Int. J. Electr. Power Energy Syst.*, vol. 134, Jan. 2022, Art. no. 107414.

[17] A. Ghasemi and M. Enayatzare, "Optimal energy management of a renewable-based isolated microgrid with pumped-storage unit and demand response," *Renew. Energy*, vol. 123, pp. 460–474, Aug. 2018.

[18] T. Xu, Y. Ren, L. Guo, X. Wang, L. Liang, and Y. Wu, "Multi-objective robust optimization of active distribution networks considering uncertainties of photovoltaic," *Int. J. Electr. Power Energy Syst.*, vol. 133, Dec. 2021, Art. no. 107197.

[19] J. Zhu, S. Huang, Y. Liu, H. Lei, and B. Sang, "Optimal energy management for grid-connected microgrids via expected-scenario-oriented robust optimization," *Energy*, vol. 216, Feb. 2021, Art. no. 119224.

[20] A. Hussain, I.-S. Choi, Y. H. Im, and H.-M. Kim, "Optimal operation of greenhouses in microgrids perspective," *IEEE Trans. Smart Grid*, vol. 10, no. 3, pp. 3474–3485, May 2019.

[21] H. Qiu, W. Gu, Y. Xu, W. Yu, G. Pan, and P. Liu, "Tri-level mixed-integer optimization for two-stage microgrid dispatch with multi-uncertainties," *IEEE Trans. Power Syst.*, vol. 35, no. 5, pp. 3636–3647, Sep. 2020.

[22] M. Mohiti, H. Monsef, A. Anvari-Moghaddam, and H. Lesani, "Two-stage robust optimization for resilient operation of microgrids considering hierarchical frequency control structure," *IEEE Trans. Ind. Electron.*, vol. 67, no. 11, pp. 9439–9449, Nov. 2020.

[23] H. Qiu, B. Zhao, W. Gu, and R. Bo, "Bi-level two-stage robust optimal scheduling for AC/DC hybrid multi-microgrids," *IEEE Trans. Smart Grid*, vol. 9, no. 5, pp. 5455–5466, Sep. 2018.

[24] M. A. Abdulgalil, M. Khalid, and F. Alismail, "Optimizing a distributed wind-storage system under critical uncertainties using benders decomposition," *IEEE Access*, vol. 7, pp. 77951–77963, 2019.

[25] B. Zeng and L. Zhao, "Solving two-stage robust optimization problems using a column-and-constraint generation method," *Oper. Res. Lett.*, vol. 41, no. 5, pp. 461–547, Sep. 2013.

[26] N. Zaree, V. Vahidinasab, and A. Estebsari, "Energy management strategy of microgrids based on benders decomposition method," in *Proc. IEEE Int. Conf. Environ. Electr. Eng. IEEE Ind. Commercial Power Syst. Eur. (EEEIC/I&CPS Eur.)*, Jun. 2018, pp. 1–6.

[27] A. Ben-Tal, A. Goryashko, E. Guslitzer, and A. Nemirovski, "Adjustable robust solutions of uncertain linear programs," *Math. Program.*, vol. 99, no. 2, pp. 351–376, 2004.

[28] M. Mohiti, H. Monsef, A. Anvari-Moghaddam, and H. Lesani, "Two-stage robust optimization for resilient operation of microgrids considering hierarchical frequency control structure," *IEEE Trans. Ind. Electron.*, vol. 67, no. 11, pp. 9439–9449, Nov. 2020.

[29] G. Liu, M. Starke, and B. Xiao, "Robust optimisation-based microgrid scheduling with islanding constraints," *IET Gener. Transm. Distrib.*, vol. 11, pp. 1820–1828, May 2017.

[30] B. Tan, H. Chen, X. Zheng, and J. Huang, "Two-stage robust optimization dispatch for multiple microgrids with electric vehicle loads based on a novel data-driven uncertainty set," *Int. J. Electr. Power Energy Syst.*, vol. 134, Jan. 2022, Art. no. 107359.

[31] B. Zhao, H. Qiu, R. Qin, X. Zhang, W. Gu, and C. Wang, "Robust optimal dispatch of AC/DC hybrid microgrids considering generation and load uncertainties and energy storage loss," *IEEE Trans. Power Syst.*, vol. 33, no. 6, pp. 5945–5957, Nov. 2018.

[32] A. Abedi and F. Romerio, "Adaptive robust vulnerability analysis of power systems under uncertainty: A multilevel OPF-based optimization approach," *Int. J. Electr. Power Energy Syst.*, vol. 134, Jan. 2022, Art. no. 107432.

[33] S. Phommixay, M. L. Doumbia, and Q. Cui, "A two-stage two-layer optimization approach for economic operation of a microgrid under a planned outage," *Sustain. Cities Soc.*, vol. 66, Mar. 2021, Art. no. 102675.

[34] Z. Li, Q. Guo, H. Sun, and J. Wang, "Sufficient conditions for exact relaxation of complementarity constraints for storage-concerned economic dispatch," *IEEE Trans. Power Syst.*, vol. 31, no. 2, pp. 1653–1654, Mar. 2016.
[35] H. Ahmadi and J. R. Martí, "Linear current flow equations with application to distribution systems reconfiguration," *IEEE Trans. Power Syst.*, vol. 30, no. 4, pp. 2073–2080, Jul. 2015.
[36] (2016). *CPLEX User Manual*. [Online]. Available: https://www.ibm.com
[37] D. Bertsimas and M. Sim, "The price of robustness," *Oper. Res.*, vol. 52, no. 1, pp. 35–53, Jan. 2004.

MILAD MANSOURI was born in Kermanshah, Iran. He received the B.S. degree in electrical engineering from the Kermanshah University of Technology, Iran, in 2018, and the M.S. degree in electrical engineering from the Bu Ali Sina University of Hamadan, Iran, in 2020. His current research interests include robust optimization, uncertainty, power management, and particularly their applications into smart/micro grids.

MOHSEN ESKANDARI was born in Saveh, Iran. He received the B.Sc. and M.Sc. degrees in electrical engineering from Islamic Azad University, Saveh Branch, Saveh, in 2004 and 2013, respectively, and the Ph.D. degree in electrical engineering from the University of Technology Sydney, Sydney, Australia, in 2021. Since March 2020, he has been a Postdoctoral Research Associate with the University of New South Wales, Sydney. He joined the AUSMURI Project as a Research Fellow, in 2021. He has more than ten years of experience in different parts of the electrical industry. He has proven skills in handling power systems projects and a strong background in the field of automation and control. His research interests include power systems, power electronics, micro/smart grids, control theory and optimization, and recently AI and navigation.

YOUSEF ASADI was born in Kermanshah, Iran. He received the B.S. degree in electrical engineering from the Razi University of Kermanshah, Iran, in 2014, and the M.S. degree in electrical engineering from the Bu Ali Sina University of Hamadan, Iran, in 2020. His current research interests include optimization, control, uncertainty, power management, and particularly their applications into smart/micro grids.

PIERLUIGI SIANO (Senior Member, IEEE) received the M.Sc. degree in electronic engineering and the Ph.D. degree in information and electrical engineering from the University of Salerno, Salerno, Italy, in 2001 and 2006, respectively. He is currently a Professor and the Scientific Director of the Smart Grids and Smart Cities Laboratory, Department of Management & Innovation Systems, University of Salerno. Since 2021 he has been a Distinguished Visiting Professor with the Department of Electrical & Electronic Engineering Science, University of Johannesburg. His research interests include demand response, energy management, the integration of distributed energy resources in smart grids, electricity markets, and planning and management of power systems. In these research fields, he has coauthored more than 660 articles, including more than 390 international journals that received in Scopus more than 14200 citations with an H-index equal to 58. In 2019, 2020, and 2021, he was awarded as a Highly Cited Researcher in engineering by Web of Science Group. He has been the Chair of the IES TC on Smart Grids. He is an Editor for the Power & Energy Society Section of IEEE ACCESS, IEEE TRANSACTIONS ON POWER SYSTEMS, IEEE TRANSACTIONS ON INDUSTRIAL INFORMATICS, IEEE TRANSACTIONS ON INDUSTRIAL ELECTRONICS, and IEEE SYSTEMS.

HASSAN HAES ALHELOU (Senior Member, IEEE) received the B.Sc. degree (Hons.) from Tishreen University, in 2011, and the M.Sc. and Ph.D. degrees (Hons.) from the Isfahan University of Technology, Iran. He is currently with the Department of Electrical and Computer Systems Engineering, Monash University, Clayton, VIC, Australia. At the same time, he is also a Professor and a Faculty Member with Tishreen University, Syria, and a Consultant with Sultan Qaboos University (SQU), Oman. Previously, he was with the School of Electrical and Electronic Engineering, University College Dublin (UCD), Dublin, Ireland, from 2020 to 2021, and Isfahan University of Technology (IUT), Iran. He was included in the 2018 & 2019 Publons and Web of Science (WoS) list of the top 1% best reviewer and researchers in the field of engineering and cross-fields over the world. He was a recipient of the Outstanding Reviewer Award for many journals, e.g., *Energy Conversion and Management* (ECM), *ISA Transactions*, and *Applied Energy*. He was a recipient of the Best Young Researcher in the Arab Student Forum Creative among 61 researchers from 16 countries at Alexandria University, Egypt, in 2011. He also received the Excellent Paper Award 2021/2022 from IEEE CSEE JOURNAL OF POWER AND ENERGY SYSTEMS (SCI IF: 3.938; Q1). He has published more than 200 research papers in high-quality peer-reviewed journals and international conferences. His research papers received more than 3000 citations with H-index of 29 and i-index of 67. He has authored/edited 15 books published in reputed publishers, such as Springer, IET, Wiley, Elsevier, and Taylor & Francis. He serves as an Editor in a number of prestigious journals, such as IEEE SYSTEMS JOURNAL, *Computers and Electrical Engineering* (CAEE) (Elsevier), *IET Journal of Engineering*, and *Smart Cities*. He has also performed more than 800 reviews for high prestigious journals, including IEEE TRANSACTIONS ON POWER SYSTEMS, IEEE TRANSACTIONS ON SMART GRID, IEEE TRANSACTIONS ON INDUSTRIAL INFORMATICS, IEEE TRANSACTIONS ON INDUSTRIAL ELECTRONICS, *Energy Conversion and Management*, *Applied Energy*, and *International Journal of Electrical Power & Energy Systems*. He has participated in more than 15 international industrial projects over the globe. His major research interests include renewable energy systems, power systems, power system security, power system dynamics, power system cybersecurity, power system operation, control, dynamic state estimation, frequency control, smart grids, micro-grids, demand response, and load shedding.